

Procedural Dataset Generation for Zero-Shot Stereo Matching

David Yan
Princeton University
yan.david@princeton.edu

Alexander Raistrick
Princeton University
araistrick@princeton.edu

Jia Deng
Princeton University
jiadeng@princeton.edu

Abstract

Synthetic datasets are a crucial ingredient for training stereo matching networks, but the question of what makes a stereo dataset effective remains largely unexplored. We investigate the design space of synthetic datasets by varying the parameters of a procedural dataset generator, and report the effects on zero-shot stereo matching performance using standard benchmarks. We collect the best settings to produce Infinigen-Stereo, a procedural generator specifically optimized for zero-shot stereo datasets. Models trained only on data from our system outperform robust baselines trained on a combination of existing synthetic datasets and have stronger zero-shot stereo matching performance than public checkpoints from prior works. We open source our system at [this URL](#) to enable further research on procedural stereo datasets.

1. Introduction

Synthetic datasets rendered by computer graphics are widely used as training data for stereo matching. Stereo matching uses a pair of RGB images to estimate per-pixel disparity, which can in turn be used to calculate scene depth. Synthetic datasets boast high quality ground truth disparity calculated using depth from the rendering pipeline. Synthetic datasets can provide stereo images for any underlying 3D graphics scene by rendering it with adjacent virtual cameras. State-of-the-art methods in stereo matching [22, 24, 41, 46, 52] all train on synthetic datasets [3, 10, 25, 38, 40, 48].

Constructing a synthetic dataset presents a myriad of design choices. How many objects should each scene contain? What types of objects should we use? How realistic must their arrangement be? What materials? What background and lighting? Synthetic datasets are often constructed using a program which makes random choices for the content of each 3D scene to maximize the diversity of the overall dataset, so in fact we must choose a *distribution* for each of these parameters. This results in an immense design space of possible scene generation programs and random distri-

butions. The best choices are not obvious - a more extreme distribution could either improve a model’s performance by making it more robust to a wider distribution, or could harm performance by diverging from real-world scenes in downstream tasks.

Early work has studied the design of synthetic datasets, helping drive progress in dataset development. Mayer et al. [26] performed a comprehensive analysis of procedural parameters for FlyingChairs [8, 17] style datasets on both disparity and flow tasks. The study’s conclusions have proved useful for research on synthetic flow datasets, inspiring later work such as AutoFlow [36]. However, Mayer et al.’s study focuses primarily on 2D flow datasets and only experiments on image augmentations for stereo data. These results do not necessarily generalize to recent stereo datasets [3, 20, 22, 38–40], which are typically rendered from 3D scenes and represent a significantly different design space. These datasets also generally do not provide ablations over generation parameters or other design decisions, making it difficult to identify what matters for downstream performance. Therefore, there remains a need for systematic analysis of synthetic datasets to further inform stereo dataset design.

In this work, we systematically explore the design space of synthetic datasets for stereo matching. Specifically, we construct a procedural dataset generator and use it to explore many possible dataset designs. For each design, we generate a stereo training dataset, use it to train a RAFT-Stereo model, then test this model to determine the effect of each dataset design. We aim to create datasets which lead to strong model performance on standard benchmarks when evaluated in zero-shot, that is, without fine-tuning on any domain-specific data. Our procedural generation system builds on top of object and scene generators Infinigen [30] and Infinigen Indoors [31], but also provides many procedural generation tools specifically designed for stereo matching data, expanding significantly upon the default options provided by the Infinigen authors.

Our study reveals a variety of interesting findings. We find that the best zero-shot stereo results come from training on a *combination* of realistic indoor scenes with added float-

ing objects. Removing realistically arranged background furniture (leaving floating objects in empty rooms) or removing the entire background (leaving just floating objects) harms zero-shot generalization. We theorize that this mixed layout is especially effective because realistic backgrounds aid real-world generalization, while the floating objects create more varied geometrical layouts and improve sample efficiency. We also find that existing stereo networks struggle to learn highly reflective and transparent materials without a substantial performance drop on diffuse regions.

We also optimize the overall computational cost of data generation. We analyze the trade-off between rendering quality and dataset cost and find that we can reduce overall GPU time for rendering from 3.37 minutes to 27 seconds per frame (7.49x) without severely impacting downstream zero-shot performance. We also created a reduced CPU-time configuration of Infinigen which reduces average runtime for each indoor scene from 50.85 minutes to 13 minutes per scene (3.9x). We then further reduce CPU cost by amortizing the cost of generating a scene over many images.

These findings lead to Infinigen-Stereo, a new procedural dataset generator which is specifically optimized for stereo matching. We use this generator to produce Infinigen-Stereo-150k, a new training dataset for stereo matching. Models trained only on this dataset achieve superior results to existing zero-shot stereo checkpoints, with a 39% reduction in error on Middlebury 2014 compared to the best prior published zero-shot checkpoint. We also compare dataset-to-dataset: our training dataset not only produces better zero-shot results than training individually on SceneFlow [25], CREStereo [22], TartanAir [40], or IRS [39], but also outperforms the same architecture trained on all these datasets *combined* by 28% on Middlebury [34] and by 25% on the Booster [32] evaluation sets. Our data is highly sample efficient: RAFT-Stereo trained on just 500 random examples from our dataset achieves lower error than 100000 CREStereo examples.

We will release Infinigen-Stereo as open-source dataset generation code, enabling anyone to generate unlimited samples from our data distribution. This constitutes the first open-source procedural generator which produces datasets that achieve strong zero-shot performance on stereo matching, and we hope it will serve as a useful tool for further customization and research.

2. Related Work

Synthetic Datasets for Stereo Matching Procedural datasets such as SceneFlow [25] typically use randomly placed flying objects in randomized backgrounds to achieve high diversity. This procedural recipe for object placement remains highly effective, with procedural datasets such as CREStereo [22] and FallingThings [38] building upon the

flying/floating object setup with additions such as photo-realistic rendering and more diverse materials. Although these datasets have been widely adopted and have had demonstrated successes in state-of-the-art stereo networks, they do not report ablations over dataset generation parameters, and therefore provide limited insight into what makes these datasets so effective. We perform detailed analysis of what procedural parameters, such as placement and material, matter most for downstream performance. Furthermore, we hypothesize that the low layout realism of existing procedural datasets leads to a large domain gap, making zero-shot generalization difficult. We draw from the successes of “floating object” style datasets and combine the floating object paradigm with realistic, procedural indoor and natural scenes.

Non-procedural synthetic datasets [2, 27] such as IRS [39], TartanAir [40], and DynamicReplica [20] rely on a limited number of realistic scenes handcrafted by 3D artists, limiting their scale and diversity. Simulators such as HS-VS [48] and VirtualKITTI [10] [3] primarily target driving sequences and lack coverage of other domains. Our dataset leverages Infinigen’s [30] [31] realistic procedural generators, allowing us to create thousands of unique indoor and natural scenes.

Procedural Generation Although there exist several open platforms for procedural data generation, there has been limited use of these platforms to produce large-scale stereo datasets. Kubric [13] generates scattered or falling objects in a 3D scene, while ProcTHOR [7] generates realistic indoor environments for embodied agent training. However, neither pipeline has demonstrated use in stereo matching. Infinigen Nature [30] and Infinigen Indoors [31] use the photorealistic Blender [5] Cycles renderer and procedurally generate realistic indoor and natural scenes. Although Infinigen has been used to generate some stereo datasets, none of them have been used to train state-of-the-art models for traditional stereo matching. Raistrick et al. [30] created a dataset using Infinigen Nature, but it did not achieve competitive performance with SceneFlow. The Infinigen-SV [19] dataset also uses video sequences from Infinigen Nature, but it is only used as a dataset to augment SceneFlow and focuses on video-consistent stereo networks. We add significant procedural randomization techniques and tune existing parameters for stereo, and are the first to demonstrate a successful Infinigen dataset for stereo matching.

Analysis of Synthetic Datasets Mayer et al. [26] perform a detailed study of the procedural generation parameters of synthetic training data for optical flow and disparity prediction. This study concludes that “realism is overrated” for effective synthetic data, motivating the further development of successful flow datasets such as AutoFlow [15, 36]. However, this study primarily studies generation parameters for FlyingChairs [8, 17] style datasets, which consist only

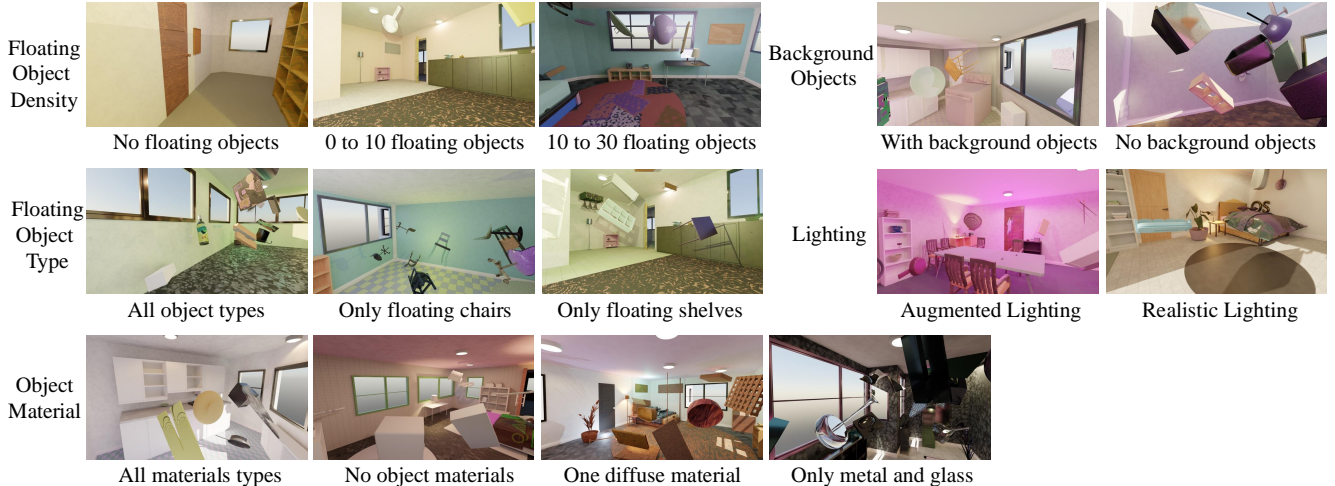


Figure 1. **Visualization of synthetic dataset design choices.** For each studied parameter, we show a single illustrative example demonstrating the effect of changing dataset generation parameters such as object density, background realism, object types, lighting, and materials. Each example is sampled from a dataset evaluated in Table 1.

of warped 2D images with no depth or disparity. Additionally, the experiments on stereo data were for augmentations simulating camera noise and blurring. As such, there is limited study of critical generation parameters, such as object placement and realism, for 3D stereo datasets. Our study focuses on stereo depth prediction, uses more realistic 3D procedural generators, and applies directly to modern stereo networks. We find that a mix of placement realism and floating objects is an effective recipe for stereo training data.

Real World Stereo Datasets Real-world datasets for stereo matching [1, 6, 9, 11, 12, 16, 28, 32–35, 44, 49] are commonly incorporated into the training sets of most stereo networks. Although real-world datasets have perfect realism, these datasets are often small or have sparse ground truth. As such, our investigation on stereo datasets focuses on synthetic datasets, which are scalable, have perfect ground truth, and allow for controlled experimentation on fine-grained features of the data.

Deep Stereo Networks Zero-shot performance is critical to a stereo network’s usability in the real-world because obtaining accurate ground truth to fine-tune for a specific use-case is often difficult and expensive. End-to-end stereo networks [4, 14, 21, 23, 25, 43, 47, 50] and iterative optimization-based networks [18, 22, 24, 41, 45, 46, 51, 52] are trained mostly on synthetic data and demonstrate impressive synthetic-to-real generalization capabilities. More details on deep stereo architectures are described in recent surveys [29, 37]. However, it remains standard practice to release separate fine-tuned checkpoints for each benchmark, and only evaluate zero-shot performance by training on SceneFlow. We demonstrate the effectiveness of our dataset by using the existing RAFT-Stereo and DLNR architectures to achieve state-of-the-art zero-shot performance,

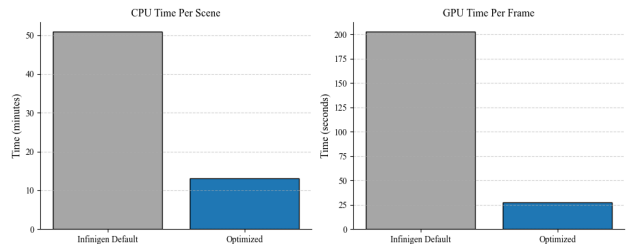


Figure 2. **Data Generation Cost Optimization.** We provide a reduced-computation configuration for Infinigen which creates acceptable indoor room arrangements with significantly reduced CPU wall-time. We also find we can use built-in OptiX denoiser to reduce GPU rendering time without severely affecting downstream stereo performance (Tab. 1). These optimizations enable significantly faster generation of large-scale datasets.

outperforming existing off-the-shelf stereo checkpoints.

3. Analysis of Dataset Parameters

3.1. Initial procedural generator

We construct our system on top of the Infinigen and Blender Python API. Infinigen provides high-level APIs to generate objects (e.g. chairs, plants, staircases, etc.) and scenes (indoors rooms, nature, or blank sky backgrounds). We directly use the Blender API to implement multiple new scene arrangement generators and other modifications which are specifically tailored to create effective stereo datasets.

Specifically, we create a floating object placement interface that calls the Infinigen API to generate objects and then arranges them throughout a given scene type. Our floating object placement has options to place objects in the view of

Experiment	Method	Middlebury 2014 (F)	Middlebury 2014 (H)	Middlebury 2021	ETH3D	KITTI-12	KITTI-15	Booster (Q)
Floating Object Density	No floating Objects	18.44	12.52	16.31	4.47	4.42	6.19	16.40
	0 to 10 floating objects	11.42	7.78	11.30	3.62	4.44	6.09	12.21
	10 to 30 floating objects	9.19	6.60	10.28	3.92	4.05	5.11	10.60
Background Objects	No background objects	10.42	8.35	12.01	4.39	4.20	6.28	12.72
	With background objects	9.19	6.60	10.28	3.92	4.05	5.11	10.60
Floating Object Type	Floating chairs	9.24	5.29	9.81	3.64	4.90	7.02	11.22
	Floating shelves	10.28	7.13	10.24	3.51	4.32	6.06	11.63
	All generators used	9.19	6.60	10.28	3.92	4.05	5.11	10.60
Object Material	No materials	11.42	9.02	10.65	3.48	4.34	6.07	14.07
	One diffuse material	10.09	7.21	9.65	2.77	3.76	5.41	12.73
	Only metal and glass	11.28	8.37	11.85	4.95	4.06	4.97	9.80
	All materials used	9.19	6.60	10.28	3.92	4.05	5.11	10.60
Stereo Baseline	Uniform[0.04, 0.1]	32.47	9.60	22.18	2.89	5.13	6.64	17.03
	Uniform[0.2, 0.3]	9.75	7.01	10.50	14.05	3.94	5.37	8.96
	Uniform[0.04, 0.4]	9.19	6.60	10.28	3.92	4.05	5.11	10.60
Ray-tracing Quality	8192 samples	8.78	6.09	9.61	3.69	9.09	10.69	11.99
	1024 samples	9.06	6.90	10.54	4.17	7.86	8.60	13.04
	1024 samples + denoising	9.19	6.60	10.28	3.92	4.05	5.11	10.6
Lighting	Realistic Lighting	9.62	6.91	10.06	3.81	3.95	5.45	10.45
	Augmented Lighting	9.19	6.60	10.28	3.92	4.05	5.11	10.60

Table 1. **Results of generation parameter study.** For each variation, we generate a new dataset of 5,000 stereo pairs and use it to train RAFT-Stereo [24]. We then report the zero-shot performance of this model on a variety of standard benchmarks. We bold the best performing models and the setting chosen for our final generator. For ray-tracing quality, we adopt *1024 samples + denoising* as our final setting despite its worse performance, as it significantly reduces dataset generation cost (Fig. 2) and allows us to construct larger scale datasets.

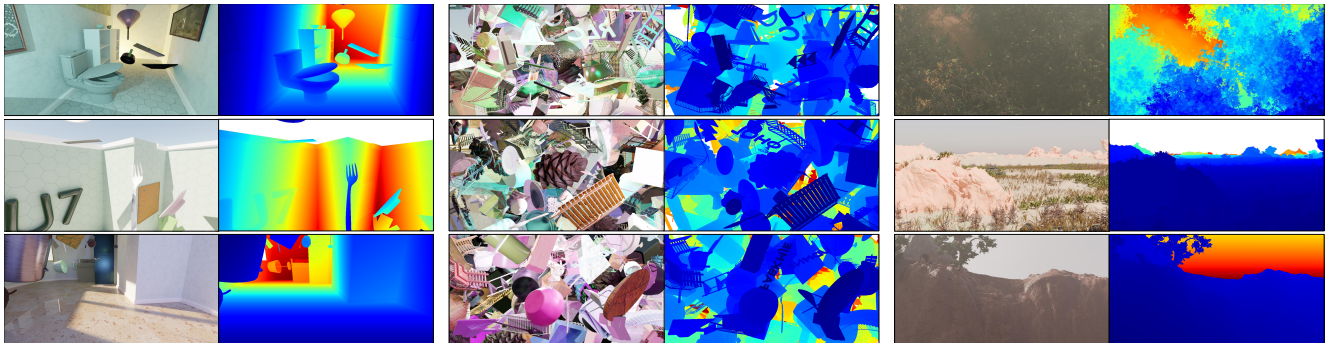


Figure 3. **Infinigen-Stereo-150k Dataset.** From left to right, we show random, non-cherrypicked samples from our *Indoors with Floating Objects*, *Dense Floating Objects*, and *Nature* scene types. Refer to the Appendix for additional samples.

a given camera through raycasting or to place objects within a specified bounding box. We also provide an option to allow floating objects to intersect existing scene geometry.

Our modifications to the Infinigen system and our floating object interface enable the system to generate three distinct scene types: indoor floating objects, dense floating objects, and nature. For the indoor floating objects scene type, we generate rooms from the Infinigen Indoor system and use our interface to generate objects at randomly sampled locations within the room’s bounding box. For the dense floating object scene type, we spawn a camera rig

in an empty sky scene and use our interface to place objects within view of the camera. Nature scenes are generated from the Infinigen Nature system.

3.2. Analysis of procedural generation parameters

We perform a systematic study to determine the effect of procedural generation parameters on zero-shot stereo matching performance. For a variety of parameters, we directly evaluate their effect on zero-shot performance. In each such case, we generate 5000 stereo pairs using the indoor floating objects scene type. We show a single illus-

Datatype	Middlebury 2014		Middlebury 2021	ETH3D	KITTI	
	(F)	(H)			2012	2015
Indoor Floating	9.19	6.60	10.28	3.92	4.05	5.11
Dense Floating	15.25	9.90	12.25	3.40	7.22	9.13
Nature	18.61	12.27	16.92	4.23	6.24	7.74
Mixed Dataset	7.81	6.04	9.29	2.51	3.54	5.12
10 - 80 - 10	10.52	6.085	10.05	2.66	3.79	4.86
80 - 10 - 10	8.13	5.90	9.21	3.01	3.81	5.31
10 - 10 - 80	9.70	7.14	10.63	2.79	3.83	5.50
33 - 33 - 33	7.81	6.04	9.29	2.51	3.54	5.12

Table 2. **Performance of different data distributions.** The top half of the table compares the performance of different scene types, where mixed denotes a dataset of equal parts indoors, dense floating. The bottom half of the table compares the performance of a mixed dataset with varying percentages for each data type. Each label denotes % Indoor - % Dense Floating - %Nature data. A mixed dataset of all dataset types is the most effective, while the indoor floating type is the best individual data type.

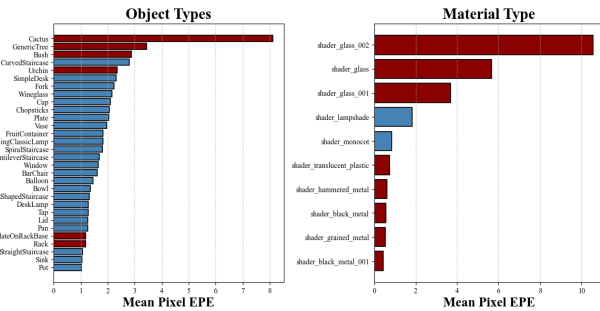


Figure 4. **End-point-error averaged by object and material.** We show average error only for the materials that make up at least 0.1% of pixels. Assets marked in red were removed from our system after manual inspection due to introducing ambiguous high-error cases, such as entirely transparent or reflective surfaces, or thin imperceptible foliage / holes.

trative example of each dataset in Fig. 1. We train RAFT-Stereo on each of these datasets for 75k steps using standard training settings. Finally, we evaluate the resulting models on the Middlebury, ETH3D, KITTI, and Booster datasets and report results in Table 1. This training setup uses both less data and a shorter training schedule to enable fast experimentation. Practically, we find that this reduced scale is sufficiently representative of the full-scale training runs.

We evaluate zero-shot performance on the Middlebury 2014 evaluation set, the Middlebury 2021 dataset, the ETH3D train set, the KITTI 2012 and KITTI 2015 train sets, and the Booster train set. For each dataset, error is defined as the percentage of pixels with end-point-error exceeding a specified threshold. The thresholds are chosen using standard ranking metrics: 2px non-occluded error for Middlebury 2014, 2px error for Middlebury 2021, 3px error for KITTI 2012 and KITTI 2015, and 2px error on Booster. We evaluate on full (F) and half (H) resolution on Middle-

bury and on quarter (Q) resolution on Booster.

Floating Object Density. Floating objects (or flying objects) are a common feature of stereo datasets. However, it is plausible that realistically arranged objects such as those produced by Infinigen Indoors would be better aligned with the distribution of real-world scenes. First, we validate whether including floating objects provide any benefit when added to scenes already containing realistic room layouts. We compare scenes with either no floating objects or 0 to 10 floating objects, and confirm that this improves Middlebury2014 (H) 2px error (12.52 to 7.78). Next, we compare this to a setting with far greater density of floating objects (uniformly sampled from 10 to 30 per scene) and again find a 2px error improvement (7.78 to 6.60). This confirms that floating objects are indeed useful and that Infinigen-Indoor scenes require additional objects to optimize for zero-shot performance. Following this result, for our dense floating object scene type, we place 200 objects in the scene to maximize object density.

Background Objects. Next, we investigate whether the furniture and other background objects (e.g. shelves, appliances) which appear in indoor scenes are useful. Such arranged objects are not present in other synthetic stereo datasets, and previous studies indicate that realism, such as these realistically placed objects, is not important [26]. However, when evaluating scenes with and without background objects, we find that including background objects *does* help, improving performance on all benchmarks (e.g. 8.35 to 6.6 2px error on Middlebury2014-H).

Object Type. We investigate to what extent the diversity of objects is useful: how helpful is sampling from all available Infinigen object generators, as opposed to using only flying chairs or shelves? Surprisingly, we find that using only Chairs actually results in small improvements on some benchmarks (Middlebury 2014 and ETH3D). However, fixing the object type to shelves results in worse performance on all benchmarks except ETH3D. These results might suggest that the diversity of the floating object meshes themselves matters less than the diversity of the arrangements and background environment. We choose to use all generators because it has the most robust performance across many benchmarks.

We also investigated objects at the level of individual object types and per-pixel errors. Specifically, we test a trained model on 1000 additional images rendered from the same procedural parameters, and we use object segmentation masks to compute average end-point-error aggregated across each object type. We plot the objects with the highest remaining error in Fig. 4. We manually inspected error maps for the highest error objects, and found objects such as cacti and urchins, which have very thin needle structures, and racks, which have very small holes. We remove these objects from use by our final system due to their extreme

Model	Middlebury 2014 (H)	Middlebury 2021	ETH3D	KITTI		Booster (Q)
				2012	2015	
PSMNet [4]	13.80	23.67	19.75	6.73	6.78	34.47
RAFT-Stereo [24]	8.66	10.28	<u>2.6</u>	4.35	5.67	17.37
IGEV [45]	11.81	20.43	43.05	7.62	7.81	23.38
GMStereo [47]	10.98	25.43	6.22	5.68	5.72	32.44
DLNR [52]	6.20	8.44	23.01	9.08	16.05	18.15
Selective-RAFT [41]	9.44	15.69	4.36	5.19	6.68	19.45
Selective-IGEV [41]	7.30	8.97	6.07	5.64	6.05	17.58
NMRF [14]	10.87	23.36	4.34	4.62	5.24	27.08
IGEV++ [46]	7.75	9.58	4.67	6.23	6.40	17.22
DLNR-Mixed	5.21	9.30	2.50	3.68	4.95	12.17
DLNR-Infinigen-Stereo-150k	3.76	6.72	2.50	<u>3.30</u>	<u>4.54</u>	9.09
RAFT-Infinigen-Stereo-150k	<u>4.48</u>	<u>8.17</u>	2.93	3.25	4.25	<u>9.17</u>

Table 3. **Zero-shot stereo results** Models trained on Infinigen-Stereo-150k outperform published methods on zero-shot stereo matching for standard evaluation benchmarks. We train DLNR-Mixed on SceneFlow, CREStereo, TartanAir, and IRS as a baseline (600k total pairs). Best results for each metric are bolded and the second best are underlined. Methods trained on our models perform better than existing zero-shot checkpoints.

difficulty.

Object Materials. We investigate the impact of various categories of materials. We applied changes to all objects except the walls to prevent very ill-posed cases such as transparent or mirror-like walls. When only glass and metallic materials are used, the model achieves the best performance on KITTI-15 and Booster, likely because these benchmarks feature many transparent or reflective surfaces, but has significantly worse performance on Middlebury and ETH3D. When just using a single diffuse material such as wood, the model obtains the best performance on Middlebury 2021, ETH3D, and KITTI 12, but does poorly on Booster, likely because of the lack of glass/metal coverage in the training data. When using no materials at all, the model performs worse across all benchmarks except ETH3D. Using a diverse array of materials results in the most robust performance across all benchmarks.

Similarly to object types, we also group per-pixel EPE by material and plot the materials with the highest error in Fig. 4. We limit this analysis to materials which comprise at least 0.1% of pixels, to prevent very rare materials (e.g. creature’s tongue / eyeball) from dominating the statistics due to low sample count. 8 of the 10 highest errors are troublesome versions of glass and metal, which are often completely transparent or completely reflective. We remove these specific materials from our system, because we find current stereo networks struggle to handle ill-posed surfaces without degrading performance on diffuse regions. However, we retain many other non-Lambertian materials which are only moderately transparent/reflective. We take particular care for external windows - replacing the glass material for these with an opaque surface would ruin light-

ing for the rest of the scene, so we instead procedurally select and delete the geometry to eliminate it from the ground truth.

Lighting Augmentation. We perform a suite of different lighting augmentations. We uniformly sample a value from 250 to 1250 watts and then evenly spread the selected wattage among 0 to 5 point lights that are randomly placed in the scene. We randomly remove the ceiling, allowing for natural sky light and highly exposed regions. We also randomly dim the ceiling lights and alter their colors to cover darker scenes. We randomize the materials of all floating and background objects.

We found that the lighting augmentations made little difference on the benchmarks, with minor improvements on Middlebury 2014 and KITTI-15, and slightly worse performance on ETH3D, Middlebury 2021, and KITTI-12. It is plausible that the lack of difference is caused by insufficient lighting variation in the benchmarks. We opt to include augmented lighting in our dataset to better account for diverse, in-the-wild lighting variations.

Stereo baseline randomization. We find that having a wide range of camera baseline values is very significant for robust generalization. When trained only on small baselines uniformly sampled between 0.04 and 0.1 meters, the model performs significantly worse across all benchmarks. When trained only on large baselines sampled between 0.2 and 0.3 m, the model’s performance improves on certain large disparity benchmarks such as Booster, but fails on small disparity benchmarks such as ETH3D. We choose to sample the baseline value uniformly from 0.04 to 0.4m, which had the best performance.

Ratio of scene types. In Table 2, we experiment on the dis-

tribution of scene types using the same experimental setup of a 5k stereo pair budget and training RAFT-Stereo for 75k steps. We find that a mixed dataset of all scene types is the most effective for stereo generalization. We also observe that indoor floating object scenes are the best individual scene type on all benchmarks except ETH3D. This result verifies the effectiveness of combining realistic scenes with floating objects over random flying objects without a background. It is likely that the dense floating object dataset performs better on ETH3D because it has lower average disparity values (since objects are further away) than indoor floating scenes.

Atmospheric effects. We disable rain, dust, and snow particles from generation because they produce valid depth values but are insufficiently visible in rendered images. Similarly, we disable the coral reef scene type because of insufficiently visible background objects.

Dataset post-processing. Certain types of undesirable scenes are hard to prevent during dataset generation, so we provide tools to remove these as a post-processing step. We use a simple mean of pixel intensities to filter out frames that are extremely dark as a result of lighting augmentation. We remove all frames with any depth value lower than a certain threshold to eliminate scenarios where the camera has clipped into an object or when an object has extremely large disparity values. For indoor scenes, this threshold is set to 12.5 cm and for nature scenes, this threshold is set to 5 meters.

3.3. Optimization of Dataset Cost

Indoor arrangement quality. Infinigen’s room solver uses a simulated annealing algorithm that iteratively adds, removes, and moves objects to optimize a set of realism constraints. However, the process by default is slow, taking on average 50.85 minutes per indoor scene on 4 Intel(R) Xeon(R) Gold 5320 CPUs. Naively reducing solver step count results in significantly sparser scenes, since the solver has fewer steps to place objects. We therefore constrain the solver to only greedily add objects, which prevents the solver from wasting steps on moving and removing objects. This approach allows for dense scenes at significantly reduced computational cost, with only a slight drop in placement realism. We decrease the number of solver steps from 550 to 60, which reduces generation times to an average of 13 minutes, shown in Figure 2.

Scene generation amortization. In order to further reduce CPU cost, we aim to extract more rendered frames from each generated scene. The base Infinigen system places a single camera within each indoor scene. Traditionally, stereo datasets will render videos from camera trajectories to obtain more frames per scene and also to obtain other useful ground truth such as optical flow. However, video sequences contain less diversity due to high overlap

between nearby frames. Because we optimize for stereo matching, we observe that frames should not be contiguous to maximize diversity. In each indoor scene, we place 20 separate stereo rigs, enforcing a minimum distance of 1m from any object. The camera locations are proposed using the default Infinigen Indoors placement algorithm, which attempts to maximize standard deviation of depth values. For our dense floating object scenes, we render 200 frame videos where object positions and orientations, lighting, and camera rig baseline values are completely randomized every single frame. These optimizations allow us to generate fewer indoor and dense floating scenes, reducing the CPU time necessary to obtain a given number of stereo frames with minimal loss of diversity.

Ray-tracing quality. We aim to optimize the GPU cost of rendering. The default Infinigen system renders using 8192 random samples per-pixel, resulting in a cost of 3.37 minutes per frame on a single NVIDIA L40 GPU. Reducing the sample count will linearly decrease render time, but results in high amounts of render noise in images. We propose the use of Blender’s Optix denoising algorithm to mitigate render noise. The denoising process results in reduced render fidelity and occasional artifacts, but our experimentation demonstrates that it is effective at improving the trade-off between render speed and render quality. We set render samples to 1024, which reduces rendering time to only 27 seconds per frame, shown in Figure 2.

We observe that, without denoising, higher render sample counts result in improved performance on all benchmarks except KITTI, suggesting that improved render quality generally improves performance. We hypothesize that the large amounts of render noise function as an augmentation that helps generalization from the indoor to driving domain, but hurts in-domain indoor performance. By applying denoising to low-sample renders, model performance generally improves across most benchmarks, demonstrating that render denoising is an effective way of mitigating performance losses caused by excessive render noise.

4. Infinigen-Stereo-150k Dataset

We use our optimized procedural generator to construct Infinigen-Stereo-150k, a stereo dataset of 152,890 stereo pairs. This dataset incorporates all the best parameter configurations found in Sec. 3. We include three categories of rendered scenes, shown in Fig. 3: indoor floating objects (69640 stereo pairs), dense floating objects (65800 stereo pairs), and nature scenes (17450 stereo pairs).

The total data generation cost was approximately 70.5 days of CPU time on 4 CPUs and 120 days of GPU time on 1 GPU. Without any of the optimizations at all, it would have taken 1902 days on 4 CPUs and 960 days on 1 GPU. In practice, we parallelize these computations over many CPUs and GPUs, drastically reducing wall-clock time to

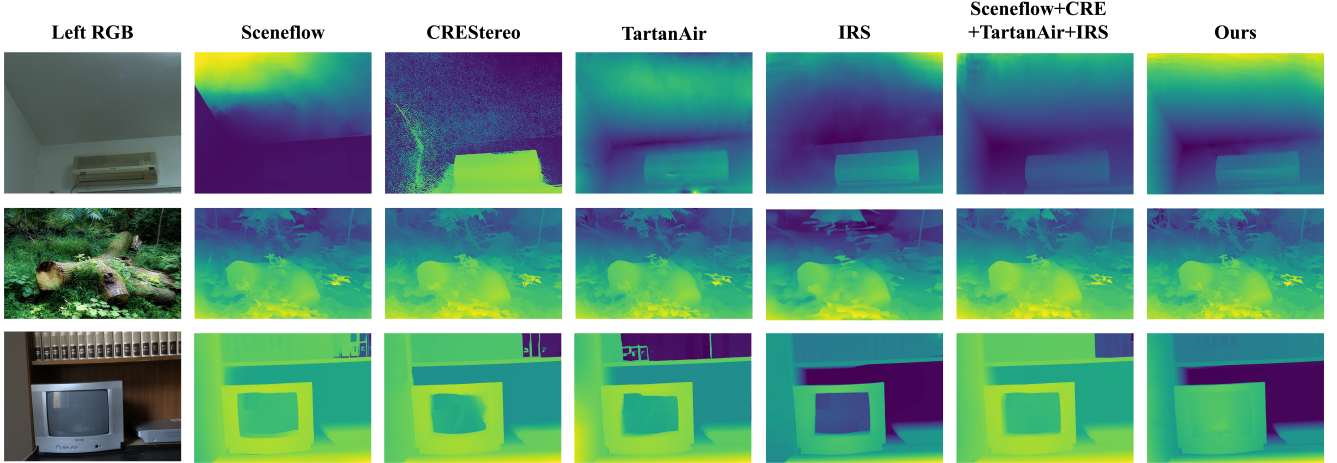


Figure 5. **Qualitative comparison of in-the-wild predictions.** We train DLNR on Infinigen-Stereo-150k and existing synthetic datasets. Training on our dataset achieves superior predictions on textureless regions (top row; blank ceiling), nature details (middle row; background leaves) and non-Lambertian surfaces (bottom row; tv screen). Images are from InStereo2k [1], Flickr1024 [42], and Booster [32].

Dataset	Middlebury 2014		Middlebury 2021	ETH3D	KITTI		Booster (Q)
	(F)	(H)			2012	2015	
Sceneflow	10.96	6.20	8.44	23.12	9.45	15.74	18.17
CREStereo	14.45	11.53	10.6	5.18	4.95	5.90	14.61
TartanAir	12.56	7.27	14.47	4.35	3.98	5.33	18.14
IRS	7.81	6.13	8.49	3.91	4.56	5.60	10.32
Infinigen-Stereo-150k	5.10	3.76	6.72	2.50	3.30	4.54	9.09

Table 4. **Zero-shot performance by dataset.** Models trained only on Infinigen-Stereo-150k outperform models trained on widely used stereo matching training datasets.

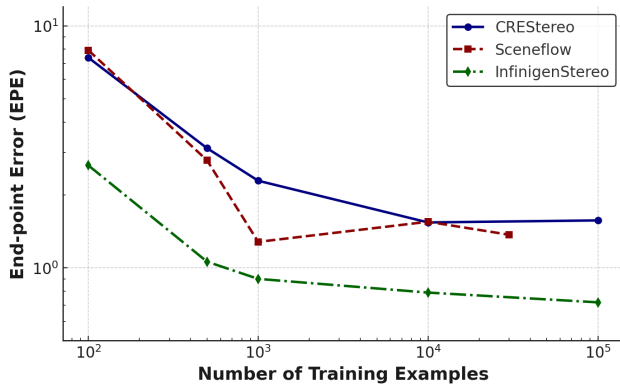


Figure 6. **Zero-shot performance by dataset budget.** Infinigen-Stereo achieves better zero-shot performance across a range of possible dataset sizes.

generate the entire dataset.

We train RAFT-Stereo and DLNR on our dataset for 200k steps, following the standard training procedures and hyperparameters used by the original authors. During train-

ing, we reweight the datasets such that each distribution type is sampled equally, following study results from 3. During training, we mask out the sky and room exteriors, which we empirically found to provide a small performance boost.

4.1. Zero-shot Generalization

Table 3 shows quantitative results on public datasets. Because most existing models are pre-trained on only Sceneflow, we retrain DLNR on a mix of Sceneflow, TartanAir, CREStereo, and IRS to provide a more robust baseline. DLNR trained on our data achieves state-of-the-art zero-shot performance across nearly all benchmarks. DLNR-Infinigen-Stereo-150k outperforms the robust baseline trained on 600k stereo pairs from a suite of existing synthetic datasets by 28% on Middlebury and by 25% on the Booster Benchmark. RAFT-Infinigen-Stereo-150k outperforms the robust baseline by 12% on KITTI 2012 and by 14% on KITTI 2015 while maintaining superior performance on Middlebury and Booster.

4.2. Qualitative Results

In Fig. 5, we compare the qualitative results of a DLNR model trained on our dataset to the same model trained on other synthetic datasets. In the first row, we observe that our model accurately predicts difficult textureless regions. In the second row, our model is able to recover fine details from a natural scene, demonstrating that our model has not overfit to indoor domains. The third row shows that our model is robust to specular regions, likely due to Infinigen-Stereo-150k’s photorealistic rendering and lighting.

4.3. Dataset comparison

We also compare our dataset individually to existing datasets. For each one of Sceneflow, CREStereo, TartanAir, and IRS, we train DLNR for 200k steps using default training settings. We report quantitative zero-shot results in Tab. 4, using metrics as defined in Sec. 3. The model trained on Infinigen-Stereo is the most robust, achieving the best performance across all benchmarks, with a 39% improvement over IRS on Middlebury 2014 (H). Despite not explicitly modeling driving scenarios, our dataset achieves better performance than Sceneflow and TartanAir (which both have driving scenes) on both KITTI-12 and KITTI-15.

We also demonstrate in Fig. 6 that Infinigen data is more effective than existing procedural datasets given the same data budget. Given a fixed dataset size, we train RAFT-Stereo for 200k steps on Infinigen-Stereo, Sceneflow, and CREStereo and evaluate their zero-shot performance on end-point error (EPE) on Middlebury half resolution. We find that Infinigen data is highly effective; just 500 training examples from Infinigen-Stereo-150k achieve a lower EPE than 100000 CREStereo training examples. Moreover our procedural “recipe” continues scaling well as the number of training examples increases, while Sceneflow plateaus at around 1000 samples and CREStereo at 10000 samples.

5. Conclusion

We contribute a thorough analysis of synthetic dataset generation for zero-shot stereo matching. We generate a new synthetic dataset and demonstrate that training solely on this dataset achieves stronger zero-shot performance than training on any previous synthetic dataset, or even on many widely used datasets combined. We believe that our study and open-source codebase will be continually useful for stereo matching research, enabling further optimization of training data in conjunction with new architectures.

6. Acknowledgments

This work was partially supported by the National Science Foundation and an Amazon Research Award.

References

- [1] Wei Bao, Wei Wang, Yuhua Xu, Yulan Guo, Siyu Hong, and Xiaohu Zhang. Instereo2k: a large real dataset for stereo matching in indoor scenes. *Science China Information Sciences*, 63:1–11, 2020. 3, 8
- [2] Daniel J Butler, Jonas Wulff, Garrett B Stanley, and Michael J Black. A naturalistic open source movie for optical flow evaluation. In *Computer Vision—ECCV 2012: 12th European Conference on Computer Vision, Florence, Italy, October 7–13, 2012, Proceedings, Part VI 12*, pages 611–625. Springer, 2012. 2
- [3] Yohann Cabon, Naila Murray, and Martin Humenberger. Virtual kitti 2. *arXiv preprint arXiv:2001.10773*, 2020. 1, 2
- [4] Jia-Ren Chang and Yong-Sheng Chen. Pyramid stereo matching network. In *Proceedings of the IEEE Conference on Computer Vision and Pattern Recognition*, pages 5410–5418, 2018. 3, 6
- [5] Blender Online Community. *Blender - a 3D modelling and rendering package*. Blender Foundation, Stichting Blender Foundation, Amsterdam, 2018. 2
- [6] Marius Cordts, Mohamed Omran, Sebastian Ramos, Timo Rehfeld, Markus Enzweiler, Rodrigo Benenson, Uwe Franke, Stefan Roth, and Bernt Schiele. The cityscapes dataset for semantic urban scene understanding. In *Proceedings of the IEEE conference on computer vision and pattern recognition*, pages 3213–3223, 2016. 3
- [7] Matt Deitke, Eli VanderBilt, Alvaro Herrasti, Luca Weihs, Jordi Salvador, Kiana Ehsani, Winson Han, Eric Kolve, Ali Farhadi, Aniruddha Kembhavi, and Roozbeh Mottaghi. ProcTHOR: Large-Scale Embodied AI Using Procedural Generation. In *NeurIPS*, 2022. Outstanding Paper Award. 2
- [8] A. Dosovitskiy, P. Fischer, E. Ilg, P. Häusser, C. Hazırbaş, V. Golkov, P. v.d. Smagt, D. Cremers, and T. Brox. FlowNet: Learning optical flow with convolutional networks. In *IEEE International Conference on Computer Vision (ICCV)*, 2015. 1, 2
- [9] Zaid A. El-Shair, Abdalmalek Abu-raddaha, Aaron Cofield, Hisham Alawneh, Mohamed Aladem, Yazan Hamzeh, and Samir A. Rawashdeh. Sid: Stereo image dataset for autonomous driving in adverse conditions. In *2024 IEEE National Aerospace and Electronics Conference (NAECON)*, 2024. 3
- [10] Adrien Gaidon, Qiao Wang, Yohann Cabon, and Eleonora Vig. Virtual worlds as proxy for multi-object tracking analysis. In *Proceedings of the IEEE conference on computer vision and pattern recognition*, pages 4340–4349, 2016. 1, 2
- [11] Andreas Geiger, Philip Lenz, and Raquel Urtasun. Are we ready for autonomous driving? the kitti vision benchmark suite. In *2012 IEEE conference on computer vision and pattern recognition*, pages 3354–3361. IEEE, 2012. 3
- [12] Jakob Geyer, Yohannes Kassahun, Mentar Mahmudi, Xavier Ricou, Rupesh Durgesh, Andrew S Chung, Lorenz Hauswald, Viet Hoang Pham, Maximilian Mühlegg, Sebastian Dorn, et al. A2d2: Audi autonomous driving dataset. *arXiv preprint arXiv:2004.06320*, 2020. 3

- [13] Klaus Greff, Francois Belletti, Lucas Beyer, Carl Doersch, Yilun Du, Daniel Duckworth, David J Fleet, Dan Gnanaprasam, Florian Golemo, Charles Herrmann, Thomas Kipf, Abhijit Kundu, Dmitry Lagun, Issam Laradji, Hsueh-Ti (Derek) Liu, Henning Meyer, Yishu Miao, Derek Nowrouzezahrai, Cengiz Oztireli, Etienne Pot, Noha Radwan, Daniel Rebain, Sara Sabour, Mehdi S. M. Sajjadi, Matan Sela, Vincent Sitzmann, Austin Stone, Deqing Sun, Suhani Vora, Ziyu Wang, Tianhao Wu, Kwang Moo Yi, Fangcheng Zhong, and Andrea Tagliasacchi. Kubric: a scalable dataset generator. 2022. 2
- [14] Tongfan Guan, Chen Wang, and Yun-Hui Liu. Neural markov random field for stereo matching, 2024. 3, 6
- [15] Hsin-Ping Huang, Charles Herrmann, Junhwa Hur, Erika Lu, Kyle Sargent, Austin Stone, Ming-Hsuan Yang, and Deqing Sun. Self-supervised autoflow. In *CVPR*, 2023. 2
- [16] Xinyu Huang, Peng Wang, Xinjing Cheng, Dingfu Zhou, Qichuan Geng, and Ruigang Yang. The apolloscape open dataset for autonomous driving and its application. *IEEE transactions on pattern analysis and machine intelligence*, 42(10):2702–2719, 2019. 3
- [17] E. Ilg, T. Saikia, M. Keuper, and T. Brox. Occlusions, motion and depth boundaries with a generic network for disparity, optical flow or scene flow estimation. In *European Conference on Computer Vision (ECCV)*, 2018. 1, 2
- [18] Junpeng Jing, Jiankun Li, Pengfei Xiong, Jiangyu Liu, Shuaicheng Liu, Yichen Guo, Xin Deng, Mai Xu, Lai Jiang, and Leonid Sigal. Uncertainty guided adaptive warping for robust and efficient stereo matching. In *Proceedings of the IEEE/CVF International Conference on Computer Vision (ICCV)*, pages 3318–3327, 2023. 3
- [19] Junpeng Jing, Ye Mao, Anlan Qiu, and Krystian Mikolajczyk. Match stereo videos via bidirectional alignment. 2024. 2
- [20] Nikita Karaev, Ignacio Rocco, Benjamin Graham, Natalia Neverova, Andrea Vedaldi, and Christian Rupprecht. Dynamicstereo: Consistent dynamic depth from stereo videos. In *Proceedings of the IEEE/CVF Conference on Computer Vision and Pattern Recognition (CVPR)*, pages 13229–13239, 2023. 1, 2
- [21] Alex Kendall, Hayk Martirosyan, Saumitro Dasgupta, Peter Henry, Ryan Kennedy, Abraham Bachrach, and Adam Bry. End-to-end learning of geometry and context for deep stereo regression. In *Proceedings of the IEEE international conference on computer vision*, pages 66–75, 2017. 3
- [22] Jiankun Li, Peisen Wang, Pengfei Xiong, Tao Cai, Ziwei Yan, Lei Yang, Jiangyu Liu, Haoqiang Fan, and Shuaicheng Liu. Practical stereo matching via cascaded recurrent network with adaptive correlation, 2022. 1, 2, 3
- [23] Zhaoshuo Li, Xingtong Liu, Nathan Drenkow, Andy Ding, Francis X. Creighton, Russell H. Taylor, and Mathias Unberath. Revisiting stereo depth estimation from a sequence-to-sequence perspective with transformers. In *Proceedings of the IEEE/CVF International Conference on Computer Vision (ICCV)*, pages 6197–6206, 2021. 3
- [24] Lahav Lipson, Zachary Teed, and Jia Deng. Raft-stereo: Multilevel recurrent field transforms for stereo matching. In *International Conference on 3D Vision (3DV)*, 2021. 1, 3, 4, 6
- [25] Nikolaus Mayer, Eddy Ilg, Philip Hausser, Philipp Fischer, Daniel Cremers, Alexey Dosovitskiy, and Thomas Brox. A large dataset to train convolutional networks for disparity, optical flow, and scene flow estimation. In *Proceedings of the IEEE conference on computer vision and pattern recognition*, pages 4040–4048, 2016. 1, 2, 3
- [26] Nikolaus Mayer, Eddy Ilg, Philipp Fischer, Caner Hazirbas, Daniel Cremers, Alexey Dosovitskiy, and Thomas Brox. What makes good synthetic training data for learning disparity and optical flow estimation? *International Journal of Computer Vision*, 126(9):942–960, 2018. 1, 2, 5
- [27] Lukas Mehl, Jenny Schmalfuss, Azin Jahedi, Yaroslava Nalivayko, and Andrés Bruhn. Spring: A high-resolution high-detail dataset and benchmark for scene flow, optical flow and stereo. In *Proc. IEEE/CVF Conference on Computer Vision and Pattern Recognition (CVPR)*, 2023. 2
- [28] Moritz Menze and Andreas Geiger. Object scene flow for autonomous vehicles. In *Proceedings of the IEEE conference on computer vision and pattern recognition*, pages 3061–3070, 2015. 3
- [29] Matteo Poggi, Fabio Tosi, Konstantinos Batsos, Philippos Mordohai, and Stefano Mattoccia. On the synergies between machine learning and binocular stereo for depth estimation from images: a survey. *IEEE Transactions on Pattern Analysis and Machine Intelligence*, 44(9):5314–5334, 2021. 3
- [30] Alexander Raistrick, Lahav Lipson, Zeyu Ma, Lingjie Mei, Mingzhe Wang, Yiming Zuo, Karhan Kayan, Hongyu Wen, Beining Han, Yihan Wang, Alejandro Newell, Hei Law, Ankit Goyal, Kaiyu Yang, and Jia Deng. Infinite photorealistic worlds using procedural generation. In *Proceedings of the IEEE/CVF Conference on Computer Vision and Pattern Recognition*, pages 12630–12641, 2023. 1, 2
- [31] Alexander Raistrick, Lingjie Mei, Karhan Kayan, David Yan, Yiming Zuo, Beining Han, Hongyu Wen, Meenal Parakh, Stamatis Alexandropoulos, Lahav Lipson, Zeyu Ma, and Jia Deng. Infinigen indoors: Photorealistic indoor scenes using procedural generation. In *Proceedings of the IEEE/CVF Conference on Computer Vision and Pattern Recognition (CVPR)*, pages 21783–21794, 2024. 1, 2
- [32] Pierluigi Zama Ramirez, Alex Costanzino, Fabio Tosi, Matteo Poggi, Samuele Salti, Stefano Mattoccia, and Luigi Di Stefano. Booster: A benchmark for depth from images of specular and transparent surfaces. *IEEE Transactions on Pattern Analysis and Machine Intelligence*, 46(1):85–102, 2024. 2, 3, 8
- [33] Daniel Scharstein and Richard Szeliski. A taxonomy and evaluation of dense two-frame stereo correspondence algorithms. *International Journal of Computer Vision*, 47(1-3): 7–42, 2002.
- [34] Daniel Scharstein, Heiko Hirschmüller, York Kitajima, Gökhan Krathwohl, Nera Nešić, Xiang Wang, and Peter Westling. High-resolution stereo datasets with subpixel-accurate ground truth, 2014. 2
- [35] Thomas Schöps, Johannes L. Schönberger, Silvano Galliani, Torsten Sattler, Konrad Schindler, Marc Pollefeys, and An-

- dreas Geiger. A multi-view stereo benchmark with high-resolution images and multi-camera videos. In *Conference on Computer Vision and Pattern Recognition (CVPR)*, 2017. 3
- [36] Deqing Sun, Daniel Vlasic, Charles Herrmann, Varun Jampani, Michael Krainin, Huiwen Chang, Ramin Zabih, William T Freeman, and Ce Liu. Autoflow: Learning a better training set for optical flow. In *CVPR*, 2021. 1, 2
- [37] Fabio Tosi, Luca Bartolomei, and Matteo Poggi. A survey on deep stereo matching in the twenties. *International Journal of Computer Vision*, 2025. 3
- [38] Jonathan Tremblay, Thang To, and Stan Birchfield. Falling things: A synthetic dataset for 3d object detection and pose estimation. In *Proceedings of the IEEE Conference on Computer Vision and Pattern Recognition Workshops*, pages 2038–2041, 2018. 1, 2
- [39] Qiang Wang, Shizhen Zheng, Qingsong Yan, Fei Deng, Kaiyong Zhao, and Xiaowen Chu. Irs: A large naturalistic indoor robotics stereo dataset to train deep models for disparity and surface normal estimation. In *2021 IEEE International Conference on Multimedia and Expo (ICME)*, pages 1–6. IEEE, 2021. 2
- [40] Wenshan Wang, DeLong Zhu, Xiangwei Wang, Yaoyu Hu, Yuheng Qiu, Chen Wang, Yafei Hu, Ashish Kapoor, and Sebastian Scherer. Tartanair: A dataset to push the limits of visual slam, 2020. 1, 2
- [41] Xianqi Wang, Gangwei Xu, Hao Jia, and Xin Yang. Selective-stereo: Adaptive frequency information selection for stereo matching. In *Proceedings of the IEEE/CVF Conference on Computer Vision and Pattern Recognition*, pages 19701–19710, 2024. 1, 3, 6
- [42] Yingqian Wang, Longguang Wang, Jungang Yang, Wei An, and Yulan Guo. Flickr1024: A large-scale dataset for stereo image super-resolution. In *Proceedings of the IEEE/CVF International Conference on Computer Vision Workshops*, pages 0–0, 2019. 8
- [43] Philippe Weinzaepfel, Thomas Lucas, Vincent Leroy, Yann Cabon, Vaibhav Arora, Romain Brégier, Gabriela Csurka, Leonid Antsfeld, Boris Chidlovskii, and Jérôme Revaud. CroCo v2: Improved Cross-view Completion Pre-training for Stereo Matching and Optical Flow. In *ICCV*, 2023. 3
- [44] Hongyu Wen, Erich Liang, and Jia Deng. Layeredflow: A real-world benchmark for non-lambertian multi-layer optical flow. *arXiv preprint arXiv:2409.05688*, 2024. Accepted to ECCV 2024. 3
- [45] Gangwei Xu, Xianqi Wang, Xiaohuan Ding, and Xin Yang. Iterative geometry encoding volume for stereo matching, 2023. 3, 6
- [46] Gangwei Xu, Xianqi Wang, Zhaoxing Zhang, Junda Cheng, Chunyuan Liao, and Xin Yang. Igev++: Iterative multi-range geometry encoding volumes for stereo matching. *arXiv preprint arXiv:2409.00638*, 2024. 1, 3, 6
- [47] Haofei Xu, Jing Zhang, Jianfei Cai, Hamid Rezatofighi, Fisher Yu, Dacheng Tao, and Andreas Geiger. Unifying flow, stereo and depth estimation. *IEEE Transactions on Pattern Analysis and Machine Intelligence*, 2023. 3, 6
- [48] Gengshan Yang, Joshua Manela, Michael Happold, and Deva Ramanan. Hierarchical deep stereo matching on high-resolution images. In *Proceedings of the IEEE/CVF Conference on Computer Vision and Pattern Recognition*, pages 5515–5524, 2019. 1, 2
- [49] Guorun Yang, Xiao Song, Chaoqin Huang, Zhidong Deng, Jianping Shi, and Bolei Zhou. Drivingstereo: A large-scale dataset for stereo matching in autonomous driving scenarios. In *Proceedings of the IEEE/CVF Conference on Computer Vision and Pattern Recognition (CVPR)*, 2019. 3
- [50] Zhichao Yin, Trevor Darrell, and Fisher Yu. Hierarchical discrete distribution decomposition for match density estimation. In *Proceedings of the IEEE/CVF conference on computer vision and pattern recognition*, pages 6044–6053, 2019. 3
- [51] Jiayi Zeng, Chengtang Yao, Yuwei Wu, and Yunde Jia. Temporally consistent stereo matching. In *Proceedings of the European Conference on Computer Vision (ECCV)*, 2024. 3
- [52] Haoliang Zhao, Huizhou Zhou, Yongjun Zhang, Jie Chen, Yitong Yang, and Yong Zhao. High-frequency stereo matching network. In *Proceedings of the IEEE/CVF Conference on Computer Vision and Pattern Recognition*, pages 1327–1336, 2023. 1, 3, 6

Appendix

A. Additional Generation Details

A.1. Indoor Floating Objects Scene Type

For each scene, we first generate the indoor scene using our modified Infinigen Indoors settings. Given this indoor scene, we place the random objects in the scene, respecting collision with existing scene objects. We then place the 20 camera rigs using the default Infinigen Indoors placement algorithm, which attempts to maximize the standard deviation of depth values. Finally, we apply augmentations as described in Section 3. We randomize the materials of all floating and background objects, replacing an object’s default material with a randomly chosen material with probability 0.5. To account for the large variance in object sizes, we normalize the floating object sizes.

A.2. Dense Floating Objects Scene Type

For each scene, we first spawn 200 objects into a scene at the origin, and use Blender’s key-frame animation system to assign each object different locations, orientation, etc. at every single keyframe. Objects were placed at a distance of Uniform(5,50) meters away from the camera and the camera baselines were sampled from Uniform(0.1, 0.4) meters. Similar to indoor scenes, we place point lights at random distances and we normalize floating object size. We rescale object size based on distance to prevent far-away objects from being completely occluded by nearby objects and apply random warping to objects. We also perform additional lighting augmentations, randomizing the sky background’s strength and color.

A.3. Nature Scene Type

We generate nature scenes with the Infinigen Nature system, using default configurations unless otherwise specified in this section and 3. By default, the Infinigen system provides configurations to render videos from a camera trajectory placed within the scene. However, these video sequences have high amounts of overlap between consecutive frames, so we render videos from camera trajectories at 6 frames per second to reduce overlap / similarity between consecutive frames. We render 50 frames from each video and sample the baseline of the stereo rig from Uniform(0.075, 0.5).

A.4. Ground Truth

For all frames, we provide camera intrinsics and extrinsics, left and right depth maps, and occlusion maps. We convert depth maps to disparity using the camera intrinsics and extrinsics. We compute occlusion maps by checking left-to-right and right-to-left re-projection consistency, with a 1 percent difference threshold. We also provide object segmentation maps, where each pixel has a value associated

with an object’s index value. Because procedural objects are never reused, we provide object names associated with each index, which enables the creation of flexible semantic segmentation maps. Similarly, materials are also procedural and never reused, so we provide material segmentation maps with material names. All frames are rendered at 1280 x 720 resolution.

A.5. List of Assets Used

Below is a list of the generators used for the floating objects.

ArmChair	Balloon
BarChair	BasketBase
Bathtub	BathroomSink
Bed	BedFrame
BeverageFridge	Blanket
BookColumn	Book
BookStack	Bottle
Bowl	Can
CeilingClassicLamp	CellShelf
Chair	Chopsticks
Cup	CurvedStaircase
DeskLamp	Dishwasher
FloorLamp	FoodBag
FoodBox	Fork
GlassPanelDoor	Hardware
Jar	KitchenCabinet
KitchenIsland	KitchenSpace
Knife	Lamp
LargePlantContainer	LargeShelf
Lid	LiteDoor
LouverDoor	Mattress
Microwave	Monitor
NatureShelfTrinkets	OfficeChair
Oven	Pallet
Pants	PanelDoor
Pillow	PlantContainer
Plate	Pot
Rug	Shirt
SimpleBookcase	SimpleDesk
Sink	SingleCabinet
Sofa	SpiralStaircase
Spoon	StraightStaircase
TableCocktail	TableDining
Tap	Towel
TriangleShelf	TV
TVStand	Vase
WallArt	Wineglass
UShapedStaircase	

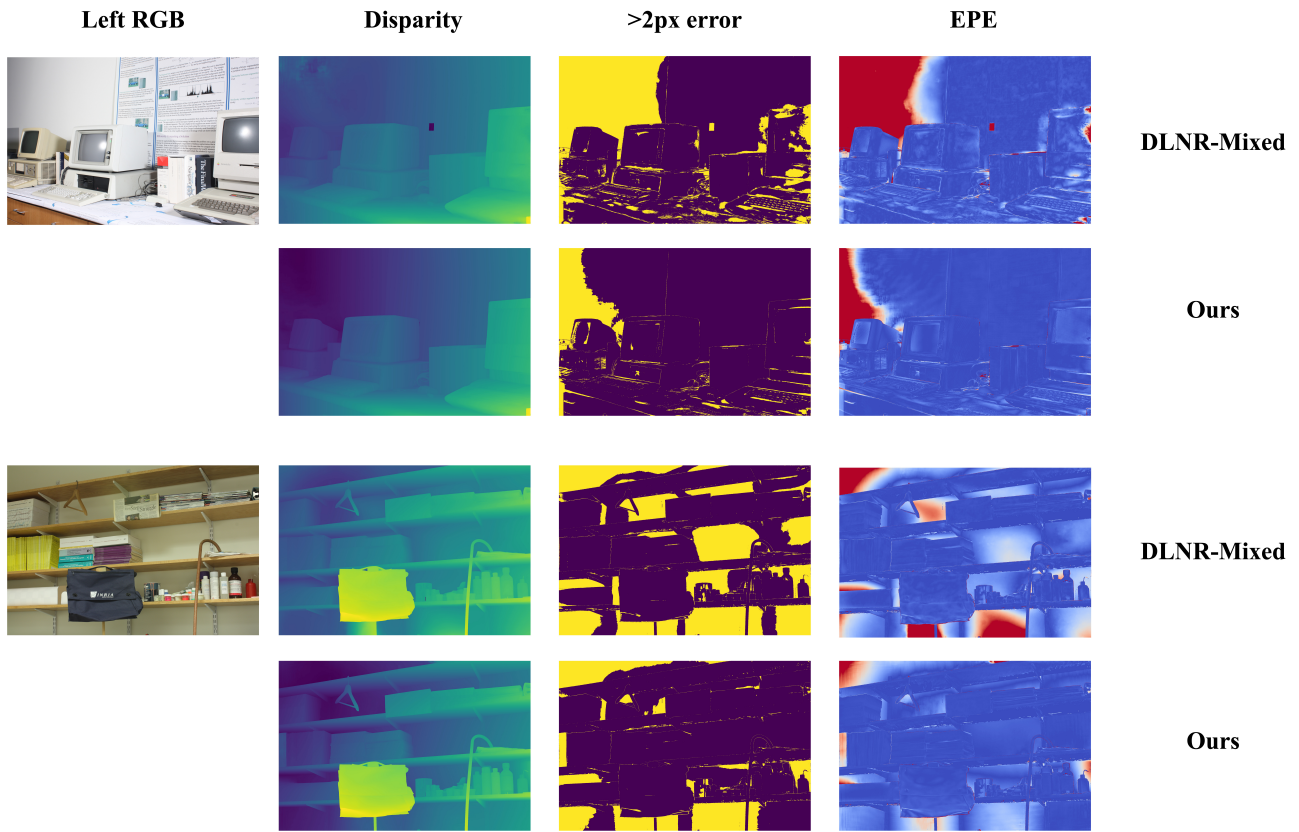


Figure 7. Qualitative results comparing DLNR-Infinigen-Stereo-150k and DLNR-Mixed on the 2014 Middlebury Eval set. Training on our dataset results in more accurate capture of walls and textureless regions.

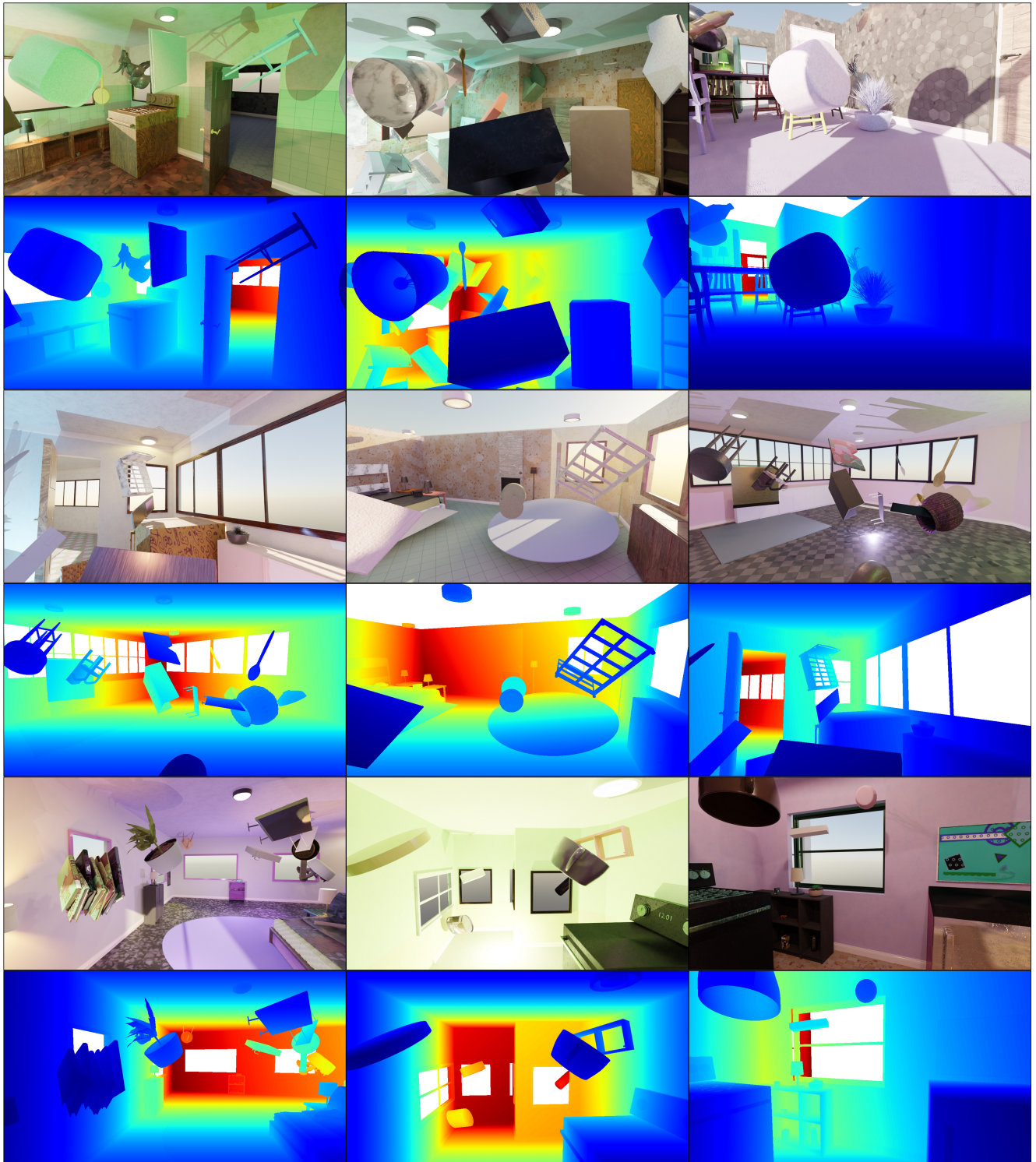


Figure 8. Non-cherrypicked, random samples from our floating indoor dataset type.

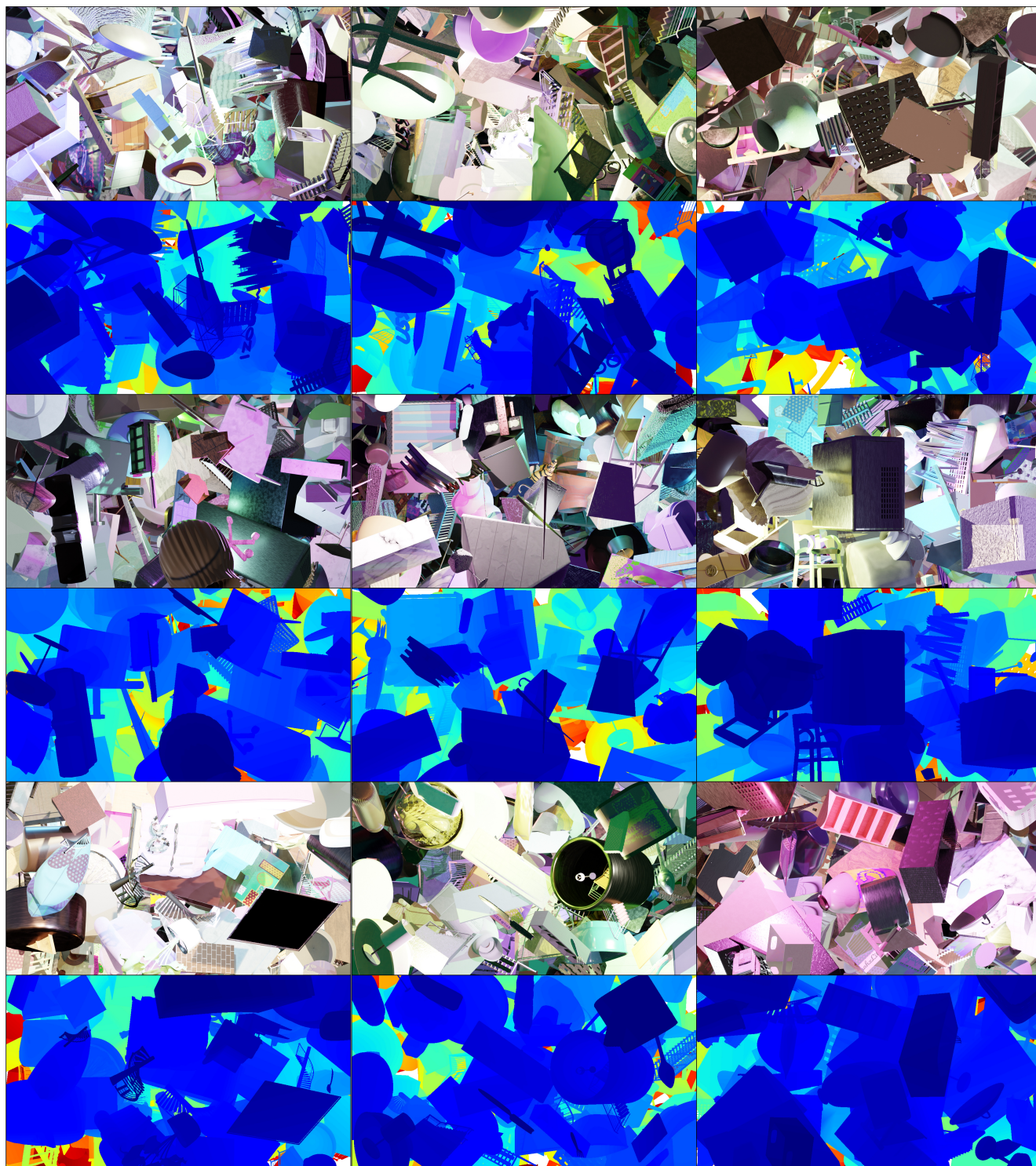


Figure 9. Non-cherrypicked, random samples from our dense floating dataset type.

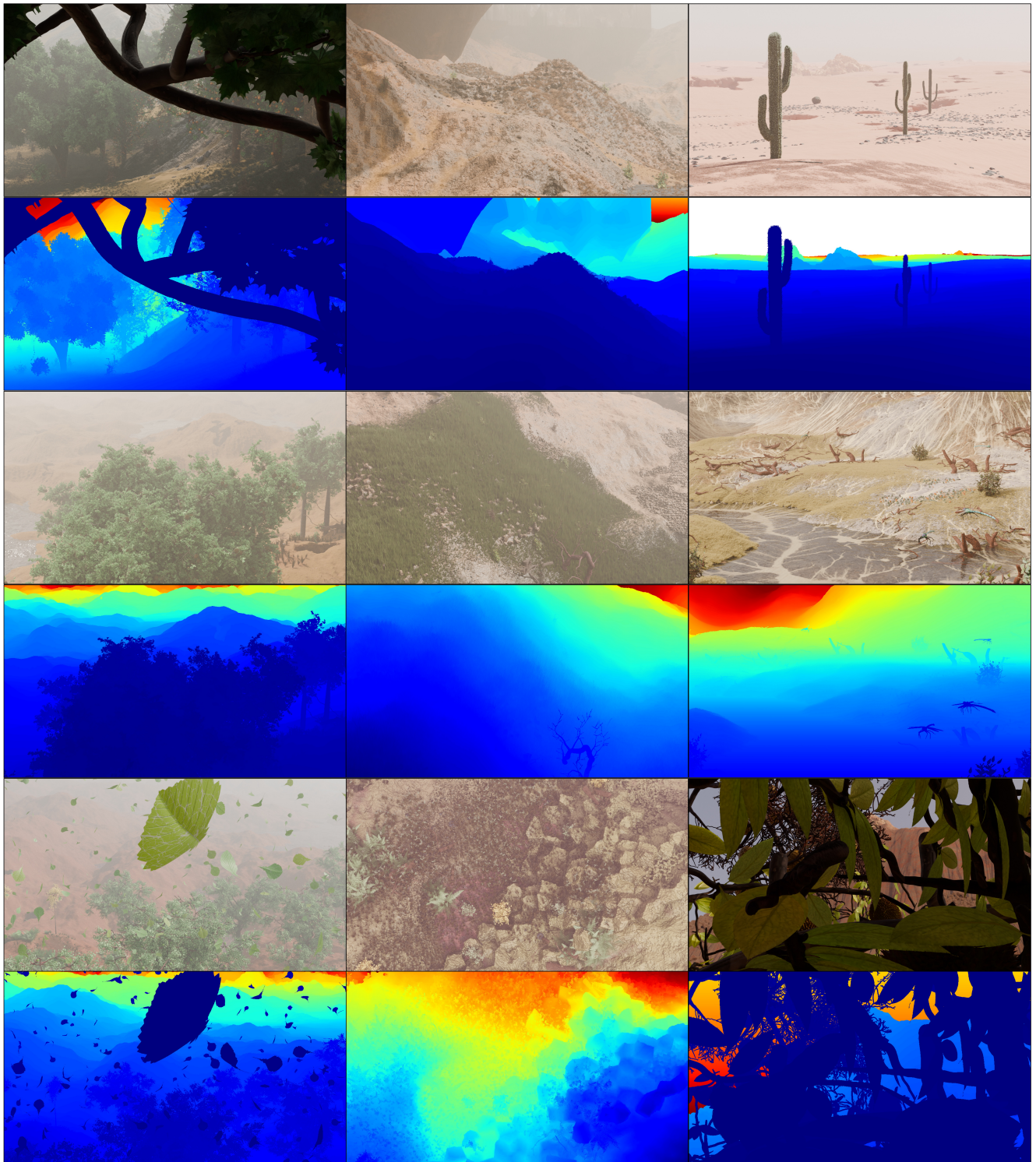


Figure 10. Non-cherrypicked, random samples from our nature dataset type.